Syntheses of Nanostructures of Cobalt Hydrotalcite Like Compounds and Co_3O_4 via a Microwave-Assisted Reflux Method

Yunshuang Ding,[†] Linping Xu,[‡] Chunhu Chen,[‡] Xiongfei Shen,[§] and Steven L. Suib*[,†,‡]

Department of Chemical, Materials and Biomolecular Engineering, University of Connecticut, 191 Auditorium Road, Unit 3222, Storrs, Connecticut 06269, Department of Chemistry, University of Connecticut, 55 North Eagleville Road, Unit 3060, Storrs, Connecticut 06269, and Intematix Inc. 46410 South Fremont Boulevard, Fremont, California 94538

Received: September 13, 2007; Revised Manuscript Received: February 19, 2008

An efficient microwave-assisted reflux route has been used to synthesize layered nanostructures of cobalt hydrotalcite like compound spheres. Scanning electron microscopy images showed that these structures are self-assemblies of the nanosheets with uniform 5-nm thickness. The layered cobalt hydrotalcite like compound has high surface area and large pore volume, which are 176 m^2/g and 1.13 m^3/g, respectively. These cobalt hydrotalcite like compounds can transfer into the spinel structure of Co_3O_4, which keeps a uniform spherical shape. Surface area and pore volume of the Co_3O_4 are 61 m^2/g and 0.5 cm^3/g, respectively. Both materials show electrocatalytic activity and stability for the electrochemical reduction of oxygen. High surface area of these catalysts correlates with high rates of electrochemical reduction of oxygen. Therefore, these materials have potential as electrocatalytic materials or as noble metal catalyst supports. This efficient route is also used to synthesize other porous transition metal oxides such as manganese oxide, nickel oxide, and others.

Introduction

3D structures of materials such as metals or transition metal oxides with controlled particle size and highly specific morphology have been of great interest to chemists and materials scientists over the past decade due to their unique properties. High surface-to-volume ratios of nanostructured materials and high density of defects result in significantly improved properties over conventional materials. For example, nanostructured catalysts with a large number of surface and edge atoms can provide a large amount of active sites for surface reactions.[1–4] Therefore, these 3D structures have many potential applications including heterogeneous catalysis,[5] batteries,[6] chemical sensors,[7] electrochromic devices,[8] and data storage.[9] Research in this area is motivated by the possibility of designing nanostructured particles that possess uniform sizes and shape distributions.

Cobalt oxides have recently been extensively studied in diverse fields. A wide range of research interest has been focused on preparation of diverse morphologies of nanostructures of Co_3O_4, such as nanotubes,[10] nanorods,[11] nanoboxes,[12] and nanocubes,[13] by using various methods including physical template methods that require droplets, silica, and block copolymer templates[14] and chemical methods including redox reactions[15] and homogeneous precipitation in normal or reverse micelles.[16] However, polymer additives are usually needed to direct the crystal growth in these methods. A variety of other methods have been developed to prepare metal oxide nanoparticles, such as sol−gel methods,[17] hydrothermal methods,[18] and sonochemical reactions,[19] which involve surfactant-assisted processes or structure-directing reagents such as polyvinylpyrrolidone (PVP)[20] or sodium dodecyl benzenesulfonate (SDBS).[21]

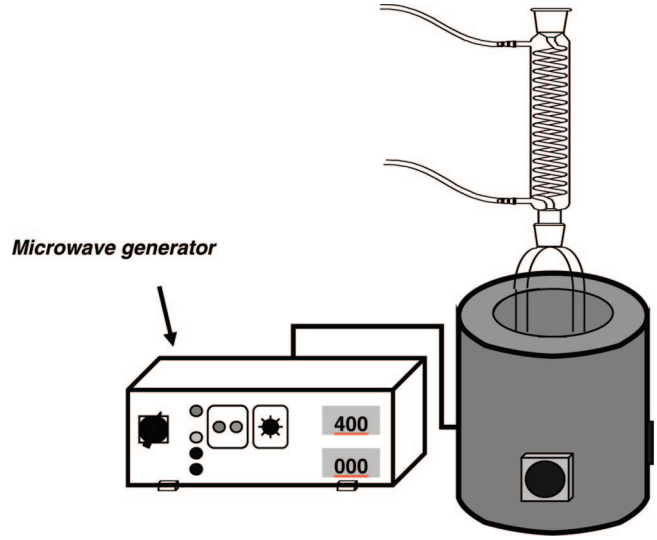

Figure 1. The schematic of microwave-assisted reflux equipments.

In most cases, the nanoparticles obtained were severely aggregated with nonuniform shape, a serious disadvantage in their applications. Therefore, it is still challenging to develop simple and efficient synthetic methods for the growth of nanostructures in an oriented way. The self-assembly method in solution has become one of the simplest synthetic routes for preparing nanosized Co_3O_4.

Studies over the past decade have demonstrated that the synthesis of nanoporous oxides may be significantly improved and extended if microwave energy is employed during the synthesis. By comparison of conventional heating methods with microwave heating, the time required for synthesis can be reduced significantly by using microwave radiation.[22] The nanomaterial products also exhibit more uniform dimensions. β-$Co(OH)_2$ nanosheets and Ultrafine $Co_{1-x}Zn_xFe_2O_4$ have been synthesized by microwave-assisted methods.[23]

* To whom correspondence should be addressed. E-mail: steven.suib@uconn.edu.
[†] Department of Chemical, Materials and Biomolecular Engineering, University of Connecticut.
[‡] Department of Chemistry, University of Connecticut.
[§] Intematix Inc.

10.1021/jp0773839 CCC: $40.75
Published on Web 05/13/2008

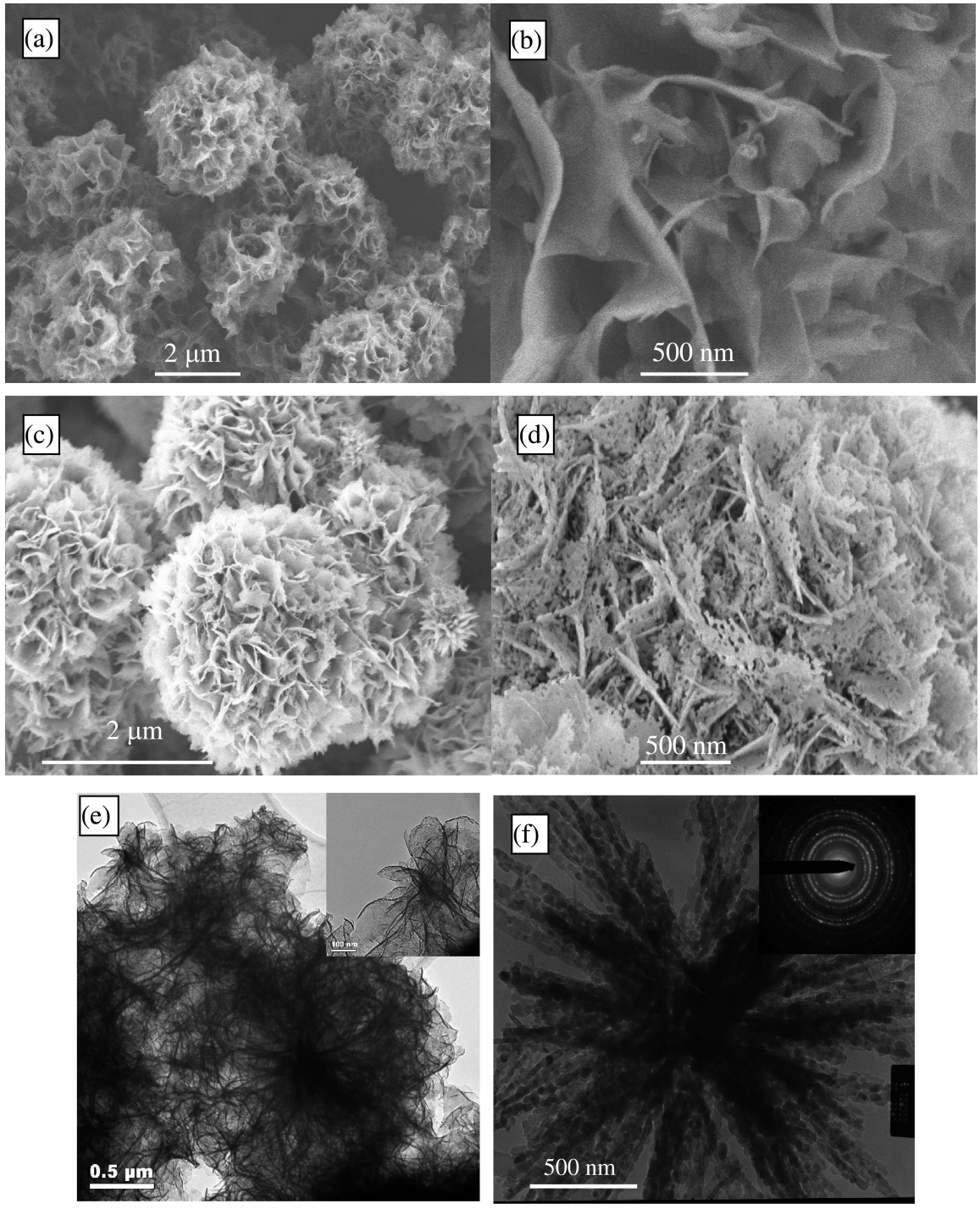

Figure 2. (a) The morphologies of HLCs before calcination. (b) FESEM image of a magnified individual flowerlike structure of the HLC. (c) The morphologies of Co_3O_4 obtained after calcination at 400 °C for 2 h. (d) FESEM image of a magnified individual flowerlike structure of Co_3O_4. (e) TEM images of HLCs before calcination. (f) TEM images of Co_3O_4 obtained after calcination at 400 °C for 2 h. Inset: selected area electron diffraction pattern of the Co_3O_4.

Hydrotalcite-like material exhibits a layer structure in which the cations show octahedral coordination. In terms of the basicity, the materials with hydrotalcite-like structure could be used as catalysts for synthesis of fine chemicals.[24] Hydrotalcite-like materials were found to have wide applications as flame retardants[25] and as anion exchangers.[26]

Herein, we report a facile microwave-assisted reflux method to prepare nanostructured cobalt hydrotalcite like compounds (HLC), in which 3D flowerlike aggregates are formed from self-assembly of extremely thin curved nanoflakes in a spontaneous process and thermal conversion to 3D flowerlike Co_3O_4 nanoparticles. No surfactants were added in this process to control the crystal growth in our experiments. The approach utilized in the present work is based on microwave synthesis of nanoparticles from metal salts in solution. Microwave irradiation (MWI) has been regarded as a very promising heating method due to several advantages over conventional methods, including short reaction time, narrow size distribution, and high purity. Because of their specific morphology, as-prepared cobalt HLCs and 3D flowerlike Co_3O_4 nanoparticles possess high surface areas (176 and 61 m^2/g, respectively) and pore volumes (1.13 and 0.5 cm^3/g, respectively). The as-obtained cobalt oxide nanomaterials

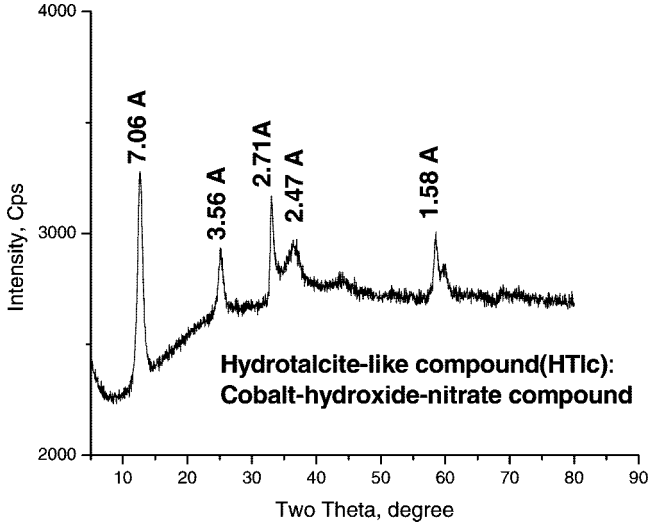

Figure 3. XRD pattern of the cobalt HLC.

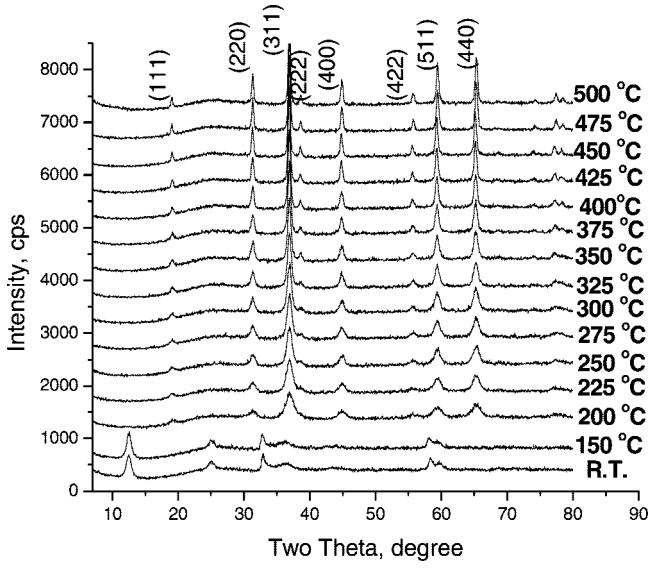

Figure 4. In situ XRD patterns of the Co_3O_4 calcined at different temperatures.

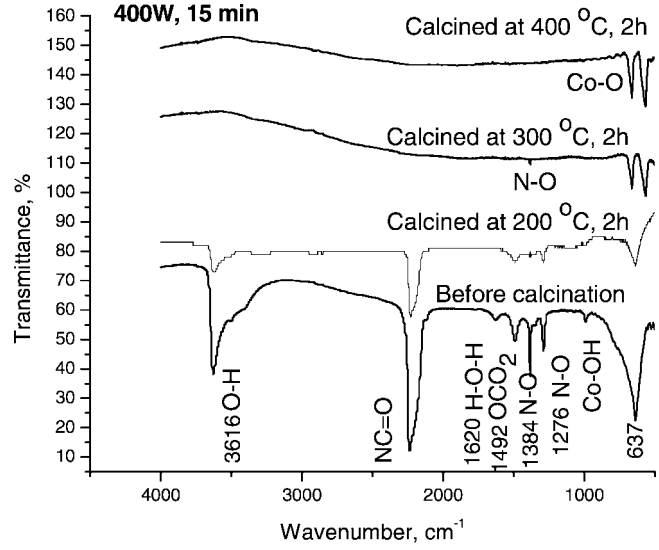

Figure 5. The FTIR spectra of cobalt HLC and the Co_3O_4 obtained after calcination.

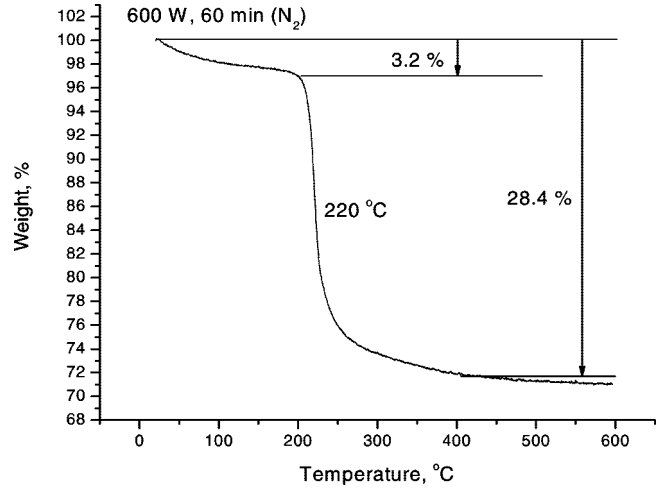

Figure 6. TGA curve of the as-obtained cobalt HLC.

have the potential to be electrocatalytic materials or as noble metal catalyst supports. This efficient route has also been used to synthesize other porous transition metal oxides such as manganese oxide and nickel oxide. The electrocatalytic activity and stability of these electrodes for the electrochemical reduction of oxygen on the cobalt HLCs and Co_3O_4 were investigated in alkaline solution.

Experimental Section

1. Syntheses of Layered Nanostructure of Cobalt HLC and Co_3O_4. The HLC precursors were prepared by microwave reflux methods that consist of a microwave power generator, a 2.45-GHz microwave oven with water circulation outside the microwave cavity, and a round-bottom tube reactor with a reflux condenser. The tube reactor is exposed to the microwaves. The schematic illustration of the setup was shown in Figure 1. In a typical experiment for the preparation, 10 mmol of cobalt nitrate, $Co(NO_3)_2 \cdot 6H_2O$ was dissolved in a mixture of 50 mL of ethylene glycol and 20 mL of deionized water. Urea (50 mmol) was then added. The resulting solution has a clear red color. This solution is transferred into a 2 foot long round-bottom tube reactor. This reactor is placed into the cavity of a microwave oven system (Wavemat Inc., Plymouth MI, USA). The top of the reactor is equipped with a water cooled condenser. The microwave power was set at 400 W, and the solution was refluxed with microwave radiation for various times (15, 30, and 90 min). The temperature of the solution is 85 °C, which is monitored with a thermocouple. The clear solution becomes opaque after 5 min of radiation. After the solution was cooled down to room temperature, the resulting pink product was collected by centrifugation and washed with deionized water and ethanol several times. The product was dried at 80 °C for 12 h. Co_3O_4 was prepared by calcining HLC precursors in a box furnace at 400 °C for 2 h, and then cooled to room temperature. Black powder was obtained for characterization.

Oxygen reduction studies were done by using cyclic voltammetry experiments. Gas-diffusion electrodes were homemade. Sample mixtures consisting of sample, carbon powder with 1:1 ratio by weight, and five drops of 25 wt % PTFE were made. The mixtures were suspended in water and sonicated. The suspensions were coated on 1 cm × 1 cm XR 72 carbon papers. The cell set up consisted of the sample mixture as a working electrode with a saturated calomel electrode (SCE) as the reference electrode and Pt as the counter electrode. The electrolytes were 1 M KOH. In a typical experiment, N_2 gas was purged through the cell for about 30 min then followed by

TABLE 1: BET Surface Areas and Total Pore Volumes of the Cobalt HLCs Prepared for Different Microwave Irradiation Time and Corresponding Calcined Co_3O_4 Samples

cobalt HLC	BET surface area (m^2/g)	total pore volume (cm^3/g)	Co_3O_4 by calcination	BET surface area (m^2/g)	total pore volume (cm^3/g)
400 W, 90 min	96	0.57	Co_3O_4	66	0.64
400 W, 30 min	99	0.54	Co_3O_4	64	0.52
400 W, 15 min	176	1.13	Co_3O_4	61	0.50

an initial scan. This was followed by 30 min of O_2 gas purge and another scan. The oxygen flow was maintained above the electrolyte during the scan to ensure saturation.

2. Characterization. Phase purity and identification of the samples were determined with X-ray diffraction (XRD) using a Scintag PDS 2000 diffractometer with a Cu Kα X-ray source ($\lambda = 1.54$ Å) in a step scan mode with a scanning rate of 0.02° s^{-1} in the 2θ range from 5 to 85° with a Cu Kα radiation source ($\lambda = 1.5418$ Å) from 5 to 80°. A Zeiss DSM 982 Gemini field emission scanning electron microscope (FESEM) with a Schottky emitter and a transmission electronic microscope (TEM) were used for morphology and microstructure studies for the synthesized materials. Samples for analysis are dispersed in ethanol and treated ultrasonically for 5 min. The resulting suspension was then dropped onto a copper grid. Structural changes of the HLCs with temperature were investigated with in situ XRD under O_2 environments in an Xtra-50 in situ X-ray diffractometer (Thermo ARL). XRD patterns were collected after the material was held at experimental temperatures (RT, 150 to 500 °C) for 0.5 h using the step scan mode with a

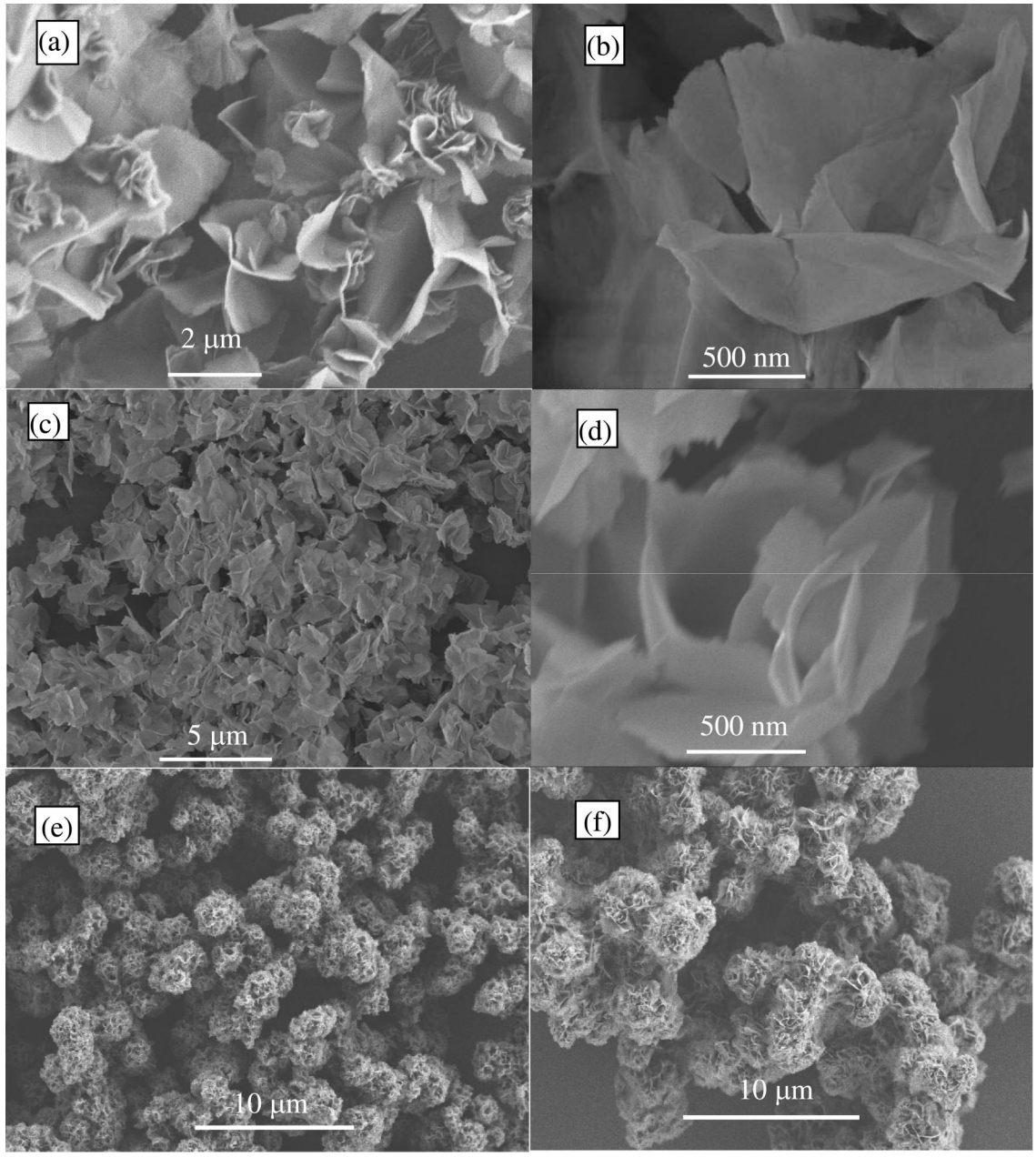

Figure 7. The morphologies of samples collected at different times (a,b) sample collected in 1 min (c,d) sample collected in 3 min (e) sample collected in 15 min (f) sample collected in 30 min.

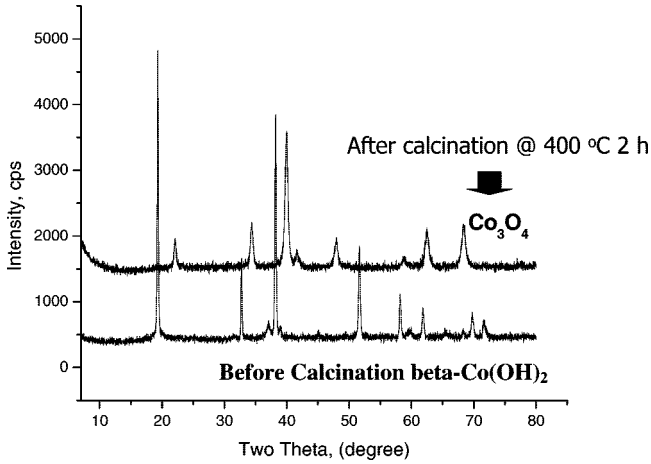

Figure 8. XRD patterns of the samples prepared using $NH_3 \cdot H_2O$ as the precipitator. (bottom) Sample before calcination; (top) sample after calcination.

scanning rate of 0.02° s^{-1} in the 2θ range from 5 to 80 °. Chemical bonding information was studied with a Fourier transform infrared (FTIR) spectrometer. About 150 mg of sample is mixed with KBr powder. The mixture is pressed into a disk for FTIR analysis. The thermal stability of the samples was studied with thermogravimetric analysis (TGA) methods. The samples were heated at a heating rate of 5 °C/min from room temperature to 600 °C in an air flow of 60 mL/min. A Micromeritics ASAP 2010 instrument was used to measure the surface areas and pore size distributions of the materials. Samples were predegassed at 120 °C for about 10 h to remove water and other physically adsorbed species. Both N_2 isothermal adsorption and desorption experiments were performed.

Results

1. Morphology and Structure. Figure 2a shows the FESEM image of typical cobalt compounds prepared for 15 min microwave irradiation time, which is composed of uniform, flowerlike architectures approximately 2−3 μm in diameter. The detailed morphology of the flowerlike nanostructures is shown in Figure 2b, which reveals that the entire structure of the architecture is built from extremely thin curved nanoflakes with smooth surfaces. These nanoflakes were estimated to be 5 nm thick and intergrow with each other to form 3D flowerlike structures. Figure 2c shows an FESEM image of the Co_3O_4 samples. The morphology of the precursor is retained after thermal treatment except that the smooth surfaces of the nanoflakes have been transferred into porous structures with a large amount of nanopores as shown in images at high magnification (Figure 2d), which are formed due to the removal of organic species in the cobalt HLC by calcination. The sizes of these nanopores ranged between 10 and 15 nm. Figure 2e shows a typical low-magnification TEM image of cobalt HLC before calcination. All the samples show flowerlike shapes with diameters of 2−3 μm, which confirms the SEM results. The images also show that the curved nanoflakes form a core congregated compactly into a flowerlike architecture. Figure 2f shows the high-resolution TEM picture of the calcined Co_3O_4 particles with a selected area diffraction pattern in the inset, which reveals the well-pronounced diffraction rings, demonstrating a polycrystalline structure.

Figure 3 shows the XRD pattern of the as-obtained cobalt compound. The diffraction peaks are similar to those of cobalt HLCs reported in the literature,[27] which can be expressed using a general formula of $M_x(OH)_y(X)_z \cdot nH_2O$ (M: metal; X: anion). The reported cobalt hydroxide nitrate compounds consist of brucite-like sheets, which results in a layered structure. Intercalation of different anions (NO_3^-, CO_3^{2-}) into the brucite-like sheets could alter the distance between the interlayer spacings in these compounds. The interlayer spacing in this cobalt HLC is 7.06 Å, which is determined from the first peak located at low angle (ca. 12°).

After the synthesis of the cobalt compounds, black power samples were obtained when we calcined the as-obtained cobalt precursors from room temperature to 500 °C. In situ XRD patterns of the calcined sample are shown in Figure 4. When the temperature was below 150 °C, the cobalt compound retains the layered structure. The Co_3O_4 phase appears when the temperature was increased to 200 °C. The intensity of all the peaks was enhanced with an increase of temperature, which means that the crystallinity of Co_3O_4 gets higher. No obvious change was observed in the XRD patterns after 400 °C. All the diffraction peaks can be indexed to the pure cubic phase of Co_3O_4 (JC-PDS 42-1467). No impurity phases have been detected.

In the FTIR spectra (Figure 5), we observed the vibrational bands of OH^- at 3616 cm^{-1}. The adsorption band observed at 1620 cm^{-1} is attributed to molecular vibrations of water interlayers. The adsorption band at 2250 cm^{-1} is assigned to the CO═N species, which provides evidence of the presence of intercalated CON^- ions in the interlayers of the compound. Bands of N—O at 1384 and 1276 cm^{-1} were also observed. The IR spectrum of the sample after calcination at 200 °C for 2 h shows similar adsorption bands with the spectrum of the uncalcined sample but lower intensity. Combined with the in situ XRD results, the organic decomposition already started at 200 °C but was not complete. Peaks around 660 and 560 cm^{-1} assigned to the υCo—O of Co_3O_4 appear after calcination at 300 °C for 2 h. When the calcination temperature reached 400 °C, only the band belonging to Co—O was retained.

2. Thermal Stability. TGA showed a small weight loss (3.2%) from room temperature to about 180 °C (Figure 6), which corresponded to the loss of structural water and part of the organic decomposition. Most of the decomposition event of the precursor happened at 220 °C. The weight loss of the precursor in this stage was 28.4%, which may be due to removal of hydroxyl, CNO^-, and carbonate anions in the sample. The TGA results are consistent with those of in situ XRD analyses.

3. Porosity. N_2 adsorption−desorption measurements were used to determine the specific surface areas and the porosities of the cobalt HLCs and Co_3O_4 materials. The surface areas and pore volumes are summarized in Table 1. The Brunauer−Emmett−Teller (BET) surface areas of the cobalt HLC were found to be 176 m^2/g for 15 min microwave irradiation time. The total pore volume is 1.13 cm^3/g, which is extremely high. An increase of the microwave radiation time to 30 and 90 min results in a decrease of surface area to 96 and 99 cm^2/g, respectively. The differences in porosity for the samples prepared at 15 min and others may be because of the existence of amorphous phases for shorter microwave irradiation time. When the microwave irradiation time increased, the crystallinity of the samples increased, which led to a decrease of surface areas. The corresponding Co_3O_4 samples prepared after calcination show similar surface areas, 61−66 m^2/g (which are higher than the BET of the commercial Co_3O_4 nanopowder, around 40 m^2/g) and pore volumes of 0.50−0.64 cm^3/g. Upon heat treatment, the HLCs were all transformed into highly crystallized Co_3O_4 phases. That is why the porosity decreased and became almost

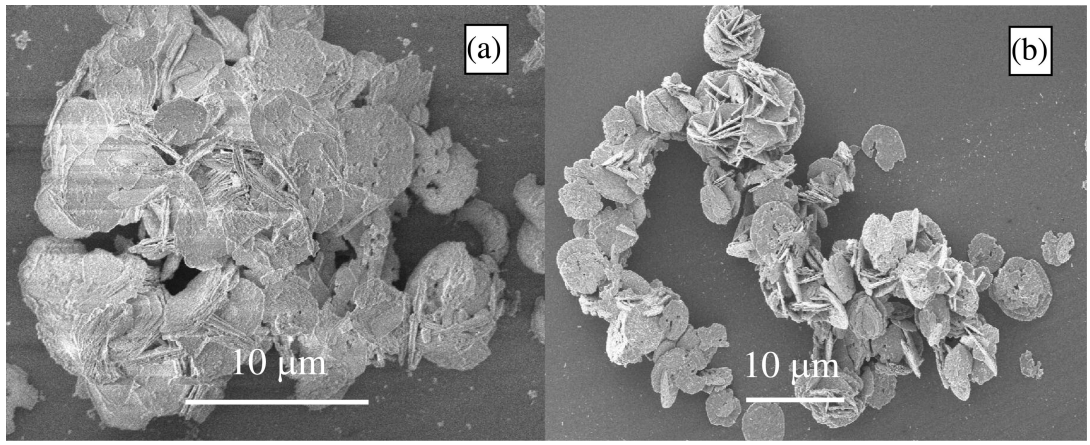

Figure 9. FESEM images of the samples prepared using $NH_3 \cdot H_2O$ as the precipitator (a) before calcination and (b) after calcination.

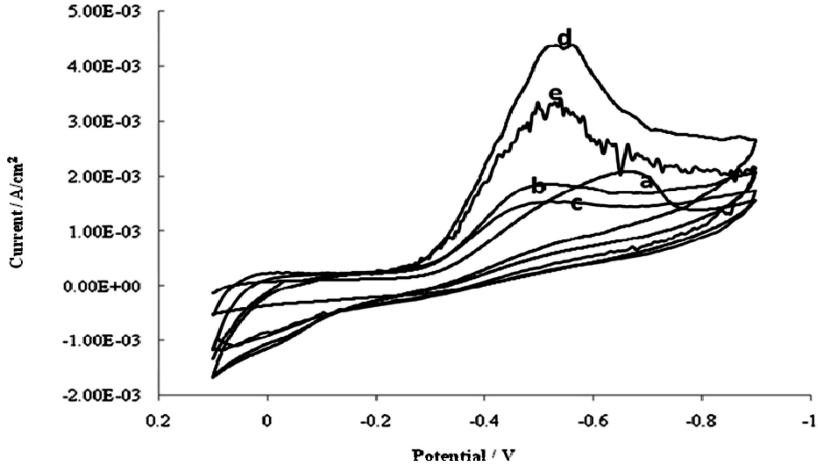

Figure 10. Cyclic voltammetry plots vs standard SCE obtained at a scan rate of 50 mV/s in 1 M KOH electrolyte for (a) blank substance of carbon powder, (b) cobalt hydroxide from ammonia system, (c) Co_3O_4 obtained after calcination of the sample in part b, (d) HLC, and (e) Co_3O_4 obtained after calcination of the sample in part d.

identical for all samples. Because of their 3D porous structure, these Co_3O_4 samples prepared by this microwave-assisted reflux followed by calcination have higher (50%) BET surface areas than commercial Co_3O_4 materials. The distribution of the pore diameters, which are derived from intervals of the nanoflakes and nanoparticles, of the cobalt HLC and Co_3O_4 are 26 and 33 nm, respectively.

To understand the crystal growth mechanism, time dependent experiments were carried out. The precipitations were collected at 1 and 3 min, respectively. The morphologies were then investigated by SEM. As shown in parts a and b of Figure 7, the cured nanoflake particles have developed even at 1 min reaction time. After 3 min, 3D flowerparts like architectures have been formed by the intergrowth of the nanoflakes (parts c and d of Figure 7). An increase in the microwave heating time to 15 and 30 min has no significant effect on particle size, but the 3D flowerlike architectures as shown in parts e and f of Figure 7 become denser than the products prepared in a short period of time.

Urea determined the crystal phase and morphology of the final product in this case. If concentrated $NH_3 \cdot H_2O$ was used as the precipitator in this process, the reaction was accelerated and prevents the formation of flowerlike superstructures. Very dilute $NH_3 \cdot H_2O$ solutions may be helpful for the formation of HLC hydroxide, as claimed in the literature.[27] XRD data (Figure 8) show that the product is β-$Co(OH)_2$. This hydroxide specie transforms to Co_3O_4 after calcination in air at 400 °C for 2 h. The prepared β-$Co(OH)_2$ and Co_3O_4 have surface areas of 48 and 39 m^2/g with similar flake morphologies, as indicated in Figure 9.

4. The Electrochemical Properties. Cyclic voltammetry experiments were performed using sample mixtures consisting of the sample, carbon powder, and PTFE in a 1:1:8 mass ratio. The sample mixtures were coated on carbon papers. Figure 9 shows the voltammograms that were obtained using 1 M KOH electrolyte. In N_2 atmosphere, the electrodes with different cobalt compounds are inactive in this potential range and with scan rates applied in these experiments. After saturation of the electrolyte with O_2, oxygen reduction potentials and peak currents were obtained, as shown in Figure 10.

Both cobalt HLC and Co_3O_4 show O_2 reduction abilities which mean they possess electrocatalytic activities as shown in Figure 10. For comparison, the electrode with blank substance (pure carbon powder) was tested, as shown in Figure 10. There is a small O_2 reduction peak observed around a potential of 0.7 V. The reduction peaks for all of the samples are almost at the same reduction potentials, around 0.5 V. Compared with the potential 0.7 V on the carbon powder electrode, O_2 is much easier to be reduced on the electrodes with these samples than on the carbon powder electrode, which means the presence of the cobalt compounds improves the activity of the carbon powder electrode. Cobalt hydrotalcite-compounds display a higher O_2 reduction peak current than Co_3O_4 samples. The products obtained from the ammonia system, both β-$Co(OH)_2$

and Co_3O_4, show less reduction current than the samples from the urea system.

Discussion

The TEM images in parts e and f of Figure 2 revealed that the surface of nanoflakes that build up the 3D structures of the cobalt hydrotalcite compound are very smooth. But these materials transform into a nanoporous structure consisting of arrays of nanoparticles interconnected together, due to the removal of hydroxyl and carbonate species in the precursor by calcination. The arrays of Co_3O_4 nanoparticles radiate from the central point of the precursor. Retention of the 3D spherical shape of Co_3O_4 can be ascribed to the shape confinement of the precursors. Another possible reason is that weak magnetic interactions between the oxide particles cause the alignment or aggregation of Co_3O_4.

The small degree of supersaturation in solution results in the heterogeneous nucleation of the metal oxide or hydroxide. When the solution undergoes supersaturation, solid particles (precipitates) are formed through nucleation and crystal growth. Ethylene glycol was used in this process to reduce the hydrolysis speed of the urea; thus precipitators like OH^- and CO_3^{2-} were released from solution slowly. Ethylene glycol acts not only as the solvent but also as a complexing agent during the growth of the nuclei. Ethylene glycol may coordinate with Co^{2+} ions to form a complex. Therefore, the nucleation of the cobalt ions proceeds slowly and the crystal growth speed can be controlled.

One of the keys to the formation of these 3D flower structures is the use of urea. Because the pH value of the primary solution (mixture of $Co(NO_3)_2$, urea, EG, and DI water) is 4.0, Co^{2+} will not be precipitated immediately. Precipitators like OH^- and CO_3^{2-} produced by urea hydrolysis deposit Co^{2+} ions slowly when the solution is heated. On the other hand, OH^- ions supplied by strong basic solution, $NH_4 \cdot OH$, will react with Co^{2+} immediately to form β-$Co(OH)_2$ precipitates.

The time-dependent experiments indicate that nucleation and crystal growth processes can be achieved rapidly. Flowerlike particles consisting of curved nanoflakes have been formed in a time frame of about a minute. The density of the nanoflakes becomes thick, and the particle size gradually grows with increase of reaction time. The formation mechanism of the final spherical morphology is still not very clear, and further investigations are ongoing. Crystal faces need attractive forces. Interfacial tension effects and hydrophilic interactions may all play an important role to drive the self-assembly of the nanoflakes into spherical structures.

Cobalt hydrotalcite compounds display a higher O_2 reduction peak current relative to Co_3O_4 samples. The results reported here show a direct relationship between the surface area and the catalytic activity. The higher surface area of the cobalt HLCs gives increased catalytically active sites toward reduction of O_2, compared to Co_3O_4 samples and β-$Co(OH)_2$. Besides surface area, the amount of hydroxyl groups is another possible influencing factor. The cobalt HLC has more hydroxyl groups than that of Co_3O_4. Both samples showed a restoration of the O_2 reduction peak when the electrolyte was repurged with O_2, indicating stability of the samples toward O_2 reduction.

Conclusions

An efficient microwave-assisted refluxing method has been used to synthesize layer structured cobalt HLCs with 3D flower like morphology via the reaction between Co^{2+} and urea. These cobalt HLCs are self-assemblies of nanoflakes and have high surface areas of 100−176 m^2/g and pore volumes of 0.54−1.13 cm^3/g. Co_3O_4 with the same spherical morphology can be obtained by calcination. The material may have promising applications in catalysis. As-synthesized cobalt hydrotalcite compounds and Co_3O_4 materials show electrocatalytic activities and can be used as electrode materials or electrocatalytic materials. Use of these materials as catalysts and syntheses of other transition metal oxides such as nickel oxides and manganese oxides using this microwave-assisted reflux method are in process.

Acknowledgment. This work was funded by the Chemical Sciences, Geo-Sciences, and Biosciences Division, Office of Basic Energy Sciences and Office of Science, U.S. Department of Energy. We also thank Linlin Zhao for his contributions in the electrochemical experiments.

References and Notes

(1) Park, S.; Lim, J. H.; Chung, S. W.; Mirkin, C. A. *Science* **2004**, *303*, 348.
(2) Shi, W. L.; Zeng, H.; Sahoo, Y.; Ohulchanskyy, T. Y.; Ding, Y.; Wang, Z. L.; Swihart, M.; Prasad, P. N. *Nano Lett.* **2006**, *6*, 875.
(3) Dujardin, E.; Mann, S. *Adv. Mater.* **2002**, *14*, 775.
(4) Zhong, L. S.; Hu, J. S.; Liang, H. P.; Cao, A. M.; Song, W. G.; Wan, L. J. *Adv. Mater.* **2006**, *18*, 2426.
(5) Yan, L.; Zhang, X.; Ren, T.; Zhang, H.; Wang, X.; Suo, J. *Chem. Commun.* **2002**, 860.
(6) Tarascon, J. M.; Armand, M. *Nature* **2001**, *414*, 359.
(7) Li, W. Y.; Xu, L. N.; Chen, J. *Adv. Func. Mater.* **2005**, *15*, 851.
(8) Nethravathi, C.; Sen, S.; Ravishankar, N.; Rajamathi, M.; Pietzonka, C.; Harbrecht, B. *J. Phys. Chem. B* **2005**, *109*, 11468.
(9) Verelst, M. T.; Ely, O.; Amiens, C.; Snoeck, E.; Lecante, P.; Mosset, A.; Respaud, M.; Brotom, J. M.; Chaudret, B. *Chem. Mater.* **1999**, *11*, 2702.
(10) Wang, R. M.; Liu, C. M.; Zhang, H. Z.; Chen, C. P.; Guo, L.; Xu, H. B.; Yang, S. H. *Appl. Phys. Lett.* **2004**, *85*, 2080.
(11) Xu, R.; Zeng, H. C. *J. Phys. Chem.* **2003**, *107*, 12643.
(12) He, T.; Chen, D.; Jiao, X.; Wang, Y. *Adv. Mater.* **2006**, *18*, 1078.
(13) Feng, J.; Zeng, H. C. *Chem. Mater.* **2003**, *15*, 2829.
(14) Steinhart, M.; Wendorff, J. H.; Greiner, A.; Wehrspohn, R. B.; Nielsch, K.; Schilling, J.; Choi, J.; Gösele, U. *Science* **2002**, *296*, 1997.
(15) Ni, Y. H.; Ge, X. W.; Zhang, Z. C. *Mater. Res. Bull.* **2001**, *36*, 2383.
(16) Harsha, V.; Colvin, V. L. *Adv. Mater.* **2000**, *12*, 833.
(17) Lakshmi, B. B.; Patrissi, C. J.; Martin, C. R. *Chem. Mater.* **1997**, *9*, 2544.
(18) Li, B.; Xie, Y.; Wu, C.; Li, Z.; Zhang, J. *Mater. Chem. Phys.* **2006**, *99*, 479.
(19) Kumar, R. V.; Diamant, Y.; Gedanken, A. *Chem. Mater.* **2000**, *12*, 2301.
(20) Chen, Y.; Zhang, Y.; Fu, S. *Mater. Lett.* **2007**, *61*, 701.
(21) (a) Hou, Y.; Kondoh, H.; Ohta, T. *Chem. Mater.* **2005**, *17*, 3994. (b) Hu, J.; Wen, Z.; Wang, Q.; Yao, X.; Zhang, Q.; Zhou, J.; Li, J. *J. Phys. Chem. B* **2006**, *110*, 24305.
(22) Tompsett, G. A.; Conner, W. C.; Yngvesson, K. S. *Chem. Phys. Chem.* **2006**, *7*, 296.
(23) (a) Liang, Z. H.; Zhu, Y. J.; Cheng, G. F.; Huang, Y. H. *Can. J. Chem.* **2006**, *84*, 1050. (b) Giri, J.; Sriharsha, T.; Bahadur, D. *J. Mater. Chem.* **2004**, *14*, 875.
(24) Lee, K. M.; Lee, W. Y. *Catal. Lett.* **2002**, *83*, 65.
(25) Adachi-Pagano, M.; Forano, C.; Besse, J. P. *J. Mater. Chem.* **2003**, *13*, 1988.
(26) Ookubo, A.; Ooi, K.; Hayashi, H. *Langmuir* **1993**, *9*, 1418.
(27) (a) Xu, R.; Zeng, H. C. *Chem. Mater.* **2003**, *15*, 2040. (b) Hosono, E.; Fujihara, S.; Honma, I.; Zhou, H. *J. Mater. Chem.* **2005**, *15*, 1938.

JP0773839